

# A New Mathematical Model for Optimum Production of Neural Stem Cells in Large-scale

S.M. Zakir Hossain<sup>1</sup>, Nahid Sultana<sup>2</sup>,  
S.M. Enayetul Babar<sup>3</sup> & G.D. Haki<sup>4</sup>

<sup>1</sup>Department of Advanced Nano and Bioscience, University of Toyama, Japan

<sup>2</sup>Department of Mathematics, Kanazawa University, Japan

<sup>3</sup>Korean Institute of Science and Technology, Cheongryang, Seoul 130-650, Korea

<sup>4</sup>Debub University, P.O.Box 05, Awassa, Ethiopia

Correspondence and requests for materials should be addressed to S.M. Enayetul Babar (babar@kist.re.kr)

Accepted 14 April 2007

## Abstract

Millions of individuals worldwide are currently afflicted with neurodegenerative disorders such as Parkinson's disease and multiple sclerosis which are caused by the death of specific types of specialized cells in the Central Nervous System (CNS). Recently, Neural Stem Cells (NSCs) are able to replace these dead cells with new functional cells, thereby providing a cure for devastating neural diseases. The clinical use of neural stem cells (NSCs) for the treatment of neurological diseases requires overcoming the scarcity of the initial *in vivo* NSC population. Thus, we developed a novel 3-dimensional cellular automata model for optimum production of neural stem cells and their derivatives in large scale to treat neurodegenerative disorder patients.

**Keywords:** Neural Stem Cells, Neurodegenerative disorder, Cellular automata model

Stem cell bioengineering is a fascinating new field that has the potential to revolutionize the practice of medicine in the 21st century. Stem cells are unspecialized master cells which reside in a particular tissue system, and can divide to give rise to all of the different specialized cell types present in that tissue. For example, it was recently determined that the central nervous system (CNS) contains neural stem cells (NSCs). These neural stem cells can divide and generate neurons, astrocytes, and oligodendrocytes which are the three primary specialized cell types that make up the CNS. The capacity of stem cells to produce

specific cell types, offers the possibility of a renewable source of replacement cells and tissues to treat chronic conditions including Huntington's disease, spinal cord injury, heart disease, and diabetes<sup>2,3,13</sup>.

NSCs in suspension culture bioreactors grow as aggregates, called neurospheres. A comprehensive study on the development of bioreactor protocols for the expansion of neurospheres in suspension bioreactors was conducted. Numerous process parameters affecting neurospheres proliferation were investigated in order to ascertain optimal operating conditions and a large body of data pertaining to the culture of these cells was consequently generated<sup>9,14-18</sup>. These studies have provided significant information to potentially develop a comprehensive mechanistic model for this particular bioreactor system. This could then provide more meaningful predictions and perhaps allow for better bioreactor design.

Models of bioreactor systems most often describe cell growth kinetics and incorporate the effects of various media constituents, such as nutrients, hormones and growth factors<sup>7,10</sup>. The most commonly used, and perhaps basic, model of cell growth follows Monod growth kinetics, which predicts the cell growth in batch conditions. Though this model describes cell growth very well for a large variety of cell cultures, it has generally been applied to bioreactors containing a single phenotype<sup>1</sup>. As a result, it may not necessarily be appropriate for heterogeneous populations, such as stem cell cultures where many different cell lines may be present at a given moment, each of which could exhibit different growth and death kinetics. In addition, Monod growth models do not necessarily take into consideration the effects of aggregate growth, which could result in increased mass transfer limitations of oxygen and other nutrients thereby inhibiting cell growth. Recently, there have been some initial efforts to simulate the fate and growth patterns of stem cells<sup>4-6,8,19,21-23</sup>. These models are only applicable to those stem cell types that do not form spheroids, or deal solely with derivatives of stem cells, and not stem cells themselves. However, it is believed that mathematical model of NSC growth might easily simulate the fate and growth pattern of stem cells within spheroids thereby a mathematical model of NSCs growth need to be developed. This could be achieved through the use of a cellular automata model in which space is represented as a uni-

form grid, time advances by steps, and the ‘laws’ are represented by a uniform set of rules which compute each cell’s state from its own previous state and those of its close neighbors. This technique had provided a means of modeling the stochastic nature of cellular reproduction in a relatively simplistic manner. Therefore, due to the simplicity of this approach, a cellular automata model was developed to model the growth of neurosphere aggregates.

The growth of neurospheres in suspension bioreactors requires detailed understanding of the dynamics NSCs within neurospheres themselves<sup>20</sup>. Since stem cell growth, self-renewal, proliferation and death are dependent upon the microscopic environment surrounding each cell, characterization of neurospheres could provide insight into this micro-environment. Given that oxygen transfer has often been considered to be the limiting factor to cell growth, characterization of cell growth within a neurosphere and the resulting oxygen concentration gradient will need to be accomplished. This had been accomplished through a mass transfer model of oxygen, based upon spherical geometries. Furthermore, neurosphere

**Table 1.** Parameters for murine neural single cells and neurospheres.

Conditions	Viable cells density, X (cells/mL)	Viability (%)	O <sub>2</sub> uptake rate, k (mol O <sub>2</sub> /cells.s)	K <sub>m</sub> (mM)
Single cells	5.38 × 10 <sup>5</sup>	92	1.22 × 10 <sup>-16</sup>	—
Neurospheres	7.4 × 10 <sup>5</sup>	96	1.09 × 10 <sup>-16</sup>	0.06

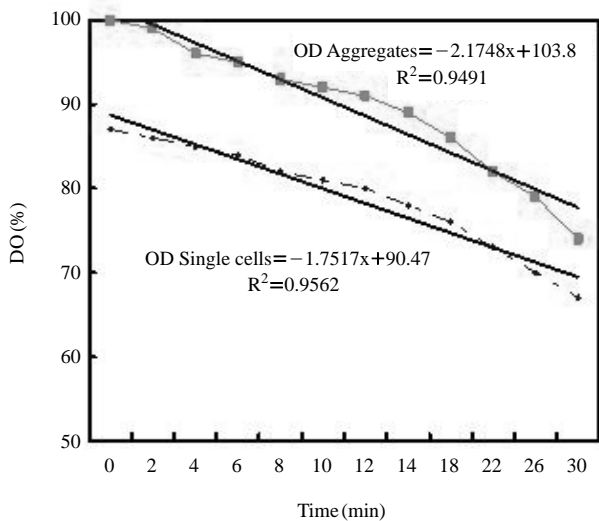


**Figure 1.** DO vs. time plots of 4-day old single cells and neurospheres/aggregates. The cells were cultured in 125 mL spinner flasks at 37°C with 5% CO<sub>2</sub> in air.

growth and the effects of NSC mobility in neurospheres were also developed through the use of a cellular automata model incorporating the effects of oxygen mass transfer. Cell viability in turn was determined by calculated the local oxygen concentration surrounding each cell.

### Determination of O<sub>2</sub> Uptake Rate and Diffusivity

The measured dissolved oxygen (DO) values of murine single cells and neurospheres, over the 30 minute experiment are shown in Figure 1. The calculated cell density, the oxygen consumption rates and other parameters for both single cells and neuros-

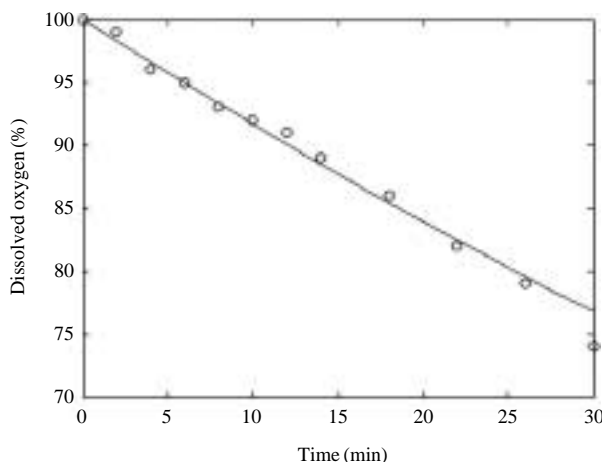


**Figure 2.** Theoretical oxygen uptake model (Solid line) was fit with experimental data (circular points) to determine a value of oxygen diffusivity through the neurosphere, assuming an average aggregate diameter of 100 μm.

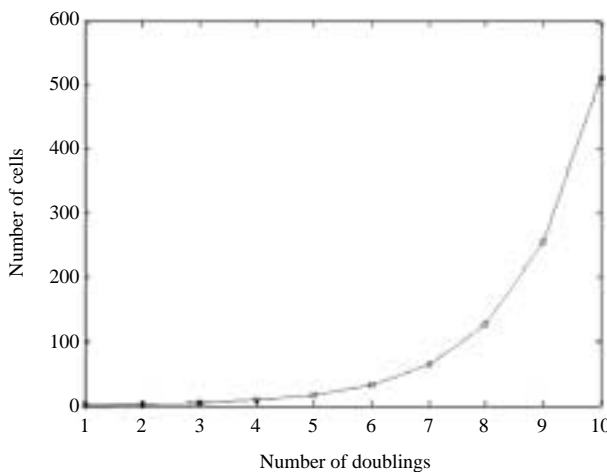


**Figure 3.** Growth curve of 1-dimensional model when all cells divide.

pheres are reported in Table 1. In Figure 2, theoretical oxygen uptake model was fit with experimental data to determine a value of oxygen diffusivity through the neurosphere, assuming an average aggregate diameter of 100  $\mu\text{m}$ . This resulted in diffusivity ( $D$ ) of  $5 \times 10^{-7} \text{ cm}^2/\text{s}$ , which was found to be in close agreement with the values found in literature for tissue aggregates<sup>15</sup>.

**Effect of O<sub>2</sub> Mass Transfer into 1-dimensional Cellular Automata Model**

The cell population doubled upon each iteration in 1-dimensional until the cell mass reached the limits of the map vector, as expected (Figure 3). In incorporation of an O<sub>2</sub> mass transfer model into the 1-dimensional cellular automata provides crucial information of oxygen availability within the aggregate. Figure 4 illustrates how rapidly oxygen can be depleted throughout the aggregate. The extent of oxygen was de-

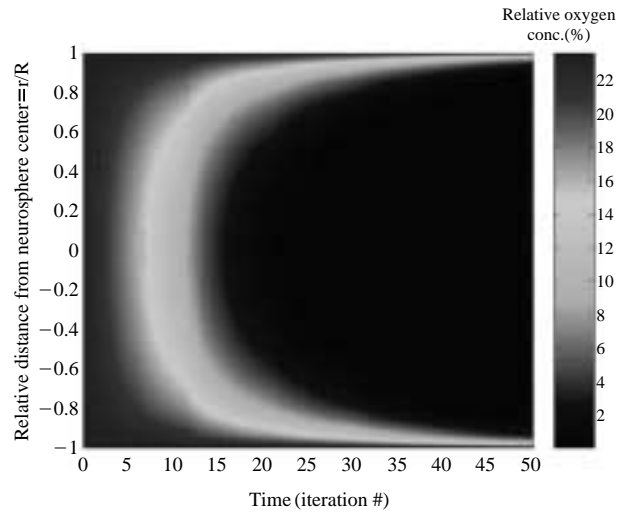


**Figure 4.** Oxygen depletion within a 1-dimensional aggregate. Cells death occurred at around 20 iterations.

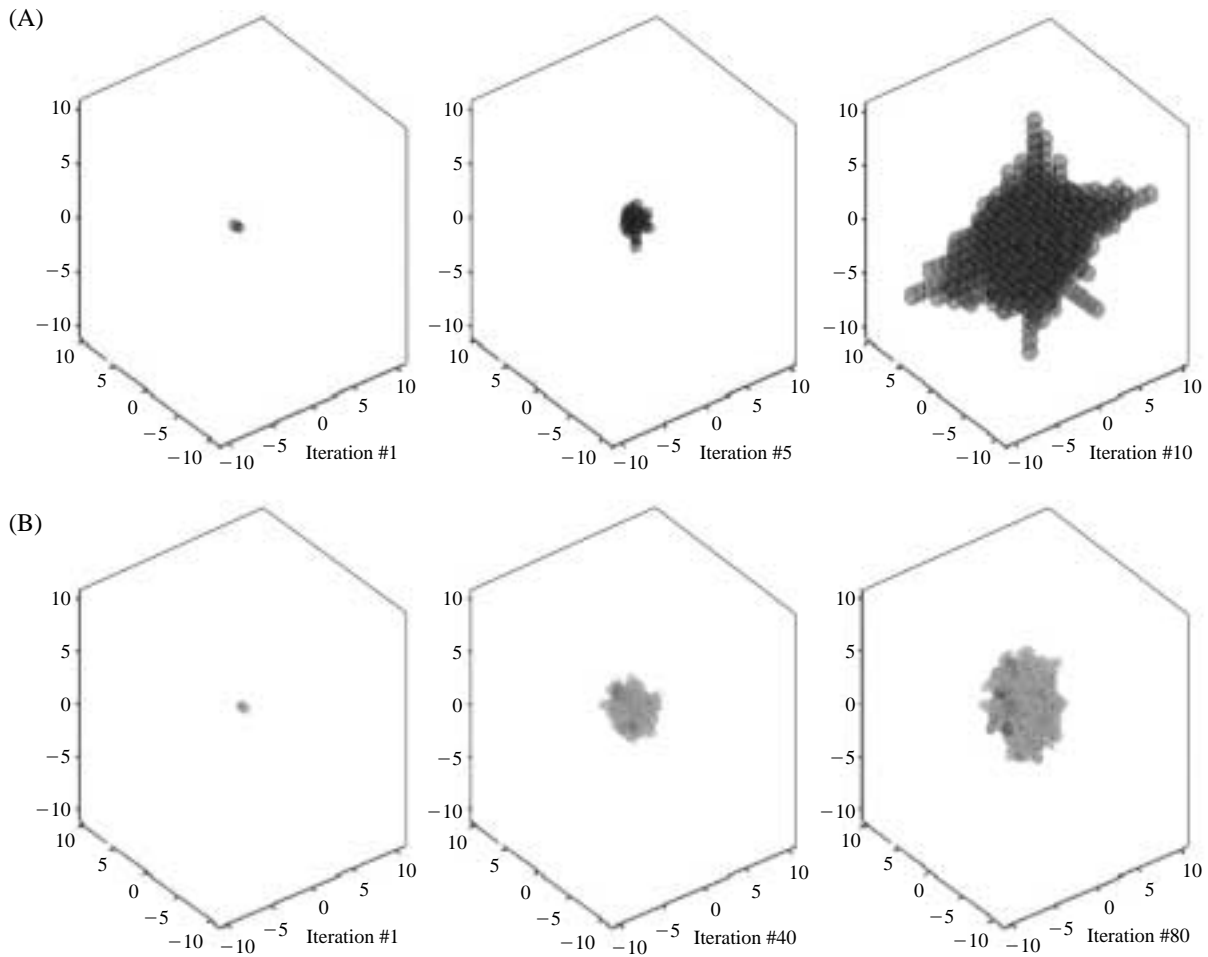


**Figure 5.** Neurosphere growth in 3-dimensional cellular automata model (A) when all cells divide (B) when only stem cells divide: red spheres denote stem cells and blue spheres denote terminally differentiated cells.

pleted as aggregates grow in size. The critical oxygen concentration, where cell death occurs due to  $O_2$  deprivation, was determined by calculating the theoretical oxygen concentration at the centre of an aggregate whose diameter is equal to the largest observed neurosphere diameter and the value was found to be  $4.82 \times 10^{-6}$  mol/L.

### Effect of $O_2$ Mass Transfer into 3-dimensional Cellular Automata Model

Adaptation of 1-dimensional displacement cellular automata rules to a 3-dimensional system resulted in an aggregate that was spherical in morphology (Figure 5A). As expected, growth curves arising from this model matched those of growth curves generated by the first 1-dimensional and 2-dimensional models developed (data not shown). With a basic 3-dimensional cellular automata model of cell growth developed, stem cell growth kinetics, cell mobility, oxygen mass transfer and cell death arising from insufficient oxygen was incorporated. It was possible to limit cell division to just stem cells using their sphere forming efficiency which have been found to be consistently 5% throughout the culture, suggesting that stem cells have an equal probability of undergoing cell death as its differentiated progeny.

Execution of the 3-dimensional model resulted in a spherical aggregate with stem cells randomly distributed throughout the neurosphere (Figure 5B). As expected, as aggregates became larger in size, a necrotic core appeared due to oxygen limitations. Oxygen concentration gradients also decreased at a much slower rate, since aggregate diameters grew more

slowly in 3-dimensions, as opposed to 1-dimension. Therefore, in Figure 6, cell death was observed apparently at around 60 iterations while in 1-dimensional system it was occurred after 20 iterations.

## Discussion

The oxygen consumption rate of single cells was significantly higher than that of the consumption rate of the aggregates. This indicated that the diffusion of oxygen into the neurospheres influenced the overall transfer of oxygen from the bulk liquid. In 2006, Wang reported that the effectiveness factor was 0.43 which suggests that the oxygen mass transfer rate into neurosphere is diffusion limiting. To determine the impact of spheroid structures on the rate of  $O_2$  diffusion into neurospheres, the diffusivity was also determined.

In 1-dimensional system, it was apparent that the majority of the aggregates were highly oxygen deprived after 20 iterations and it was unlikely that any cell would remain viable in such conditions. It is important to note that the cellular automata model was based upon 1-dimensional cell growth and the mass transfer model was based upon a 3-dimensional sphere. As a result, the appearance of a hypoxic centre after 20 doublings is likely premature. This is because the rate at which the aggregate diameter increases is directly proportional to the number of cells present for a 1-dimensional system, while in a 3-dimensional system, aggregate diameter would be proportional to the cube root of cell number.

The use of a 3-dimensional mass transfer model to a 3-dimensional cellular automata model, allowed for the correct determination of oxygen concentration gradients with respect to cell doublings. This in turn, provided a means of accurately characterizing neurosphere growth and cell death resulting oxygen deprivation. The cell viability was determined by killing off cells whose oxygen availability was less than the critical oxygen concentration.

Sphere forming efficiency also had an effect upon the behavior of the growth curve. At exceptionally low sphere forming efficiencies, a greater number of cell doublings were required to produce an equivalent number from those produced at higher sphere forming efficiencies. Additionally, at 0% sphere forming efficiencies, the growth curve was linear since only one terminally differentiated cell was produced at every cell division. As expected, when sphere forming efficiencies were set to 100% (i.e. only stem cell are produced), the model reduced to the previous 1-dimensional model where all cells divided. There has

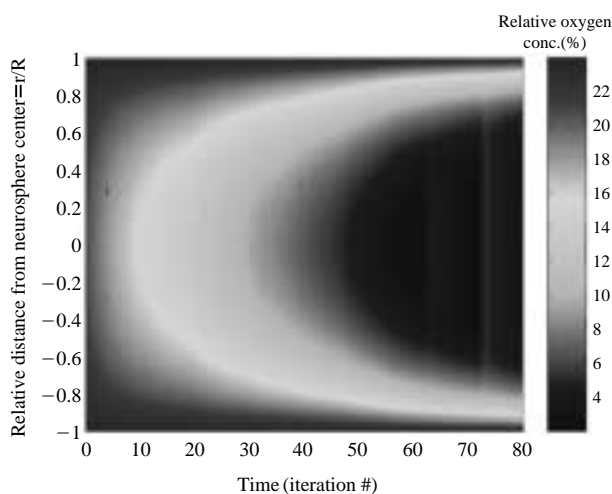


**Figure 6.** Oxygen depletion within a 3-dimensional neurosphere. Unlike the 1-dimensional model, cell death occurred at around 60 iterations as opposed to 20.

been recent evidence to suggest that cells within neurospheres are highly motile, which could result in equalizing the likelihood of cell death between stem cells and differentiated cells. The effect of cell motility was incorporated by randomly swapping locations of viable cells within the neurosphere following each cell doubling.

In summary, this study was involved both experimental research in the laboratory, and the development of a theoretical framework to use these experimental results. In the process of developing a 3-dimensional cellular automata model for neurosphere growth, a more detailed understanding of this system was gained. The development of a mass transfer model for oxygen resulted in the determination of oxygen diffusivity, which was not previously known. In determining oxygen diffusivity, theoretical oxygen concentrations could be determined for any given aggregate diameter. This in turn allowed for the calculation of a critical oxygen concentration. With this information it was possible to follow the growth of the necrotic core as the neurosphere grew. The effects of cell mobility were incorporated into the model to equalize the probability of cell death between stem cells and differentiated cells. The lessons learned in the 1-dimensional system, was then applied successfully to a more complicated 3-dimensional system. Thus, the development of this model should help facilitate our understanding of neurospheres cultures in suspension bioreactors and thereby help to optimize the production of neural stem cells and their derivatives in large scale for clinical applications.

## Methods

### Model Development

To get a realistic characterization of neurospheres growth, development of 3-dimensional cellular automata model is necessary. Before a 3-dimensional model could be made, 1-dimensional and 2-dimensional models of cell division were developed to ameliorate possible complications arising from additional dimensions. Matlab (version 6.1) was used for code generation.

### 1-dimensional Cellular Automata Model-When All Cells Divide

The simplest system that can be modeled through cellular automata is cell division along one dimension. In such a system, all cells undergo cellular division for each time interval, displacing its neighbors upon the cell division. As time progresses, a linear colony of cells increases in length exponentially,



**Figure 7.** Upon mitosis *B. subtilis* undergoes cell division so that the daughter cells are attached at the ends of each other which resemble one-dimensional growth.

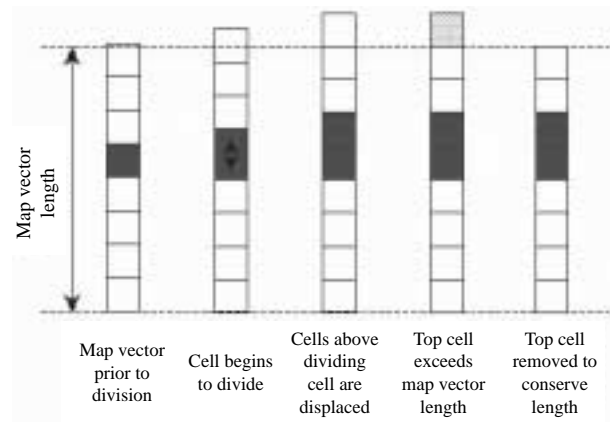


**Figure 8.** Conservation of map vector length after cell division.

closely resembling the normal growth of certain bacteria such as *Bacillus subtilis* (Figure 7).

For 1-dimensional model development, a 1-dimensional vector of set length generates discretized space. Each element within the vector denotes a specific node. For the model, this vector is called the map vector. The map vector provides information on whether or not a node is occupied by a cell. The vector element corresponding to the occupied nodes would have a value of 1, while unoccupied nodes would exhibit a value of 0. Thus, the map vector provides information on cell location. Cell displacement can be achieved by inserting the new cell produced by cell division between the old cell and its adjacent cell and shifting all the remaining cells accordingly. The displaced element at the end of the map vector is remov-

ed to ensure the length of the map vector remains constant (Figure 8).

### 2-dimensional Cellular Automata Model-When Only Stem Cells Divide

Only small number of cells (i.e. stem cells) within the aggregate is capable of proliferating. To incorporate the presence of stem cells in the neurosphere, a vector similar to the map vector is made. Like the map vector, the stem-map vector describes the location of stem cells through 1's and 0's. As a result, the localization of stem cells within the cell population can be followed. In addition, an address for a specific cell within the stem-map vector will be equivalent to the cell's address in the map vector. The code for the previous 1-dimensional model is slightly modified by incorporating a probability factor (sphere forming efficiency of stem cells) so that only stem cells are capable of cell division.

### 3-dimensional Cellular Automata Model for Stem Cells

Rules of cell displacement developed for the 1-dimensional system is adapted first to a 2-dimensional system and then into 3-dimensional system to get a comprehensive model for neurospheres growth. The effects of oxygen mass transfer, cell mobility and cell death arising from insufficient oxygen are incorporated. As aggregates increase in size, mass transfer limitations of nutrients become more significant, potentially inhibiting cell proliferation and viability. Moreover, concentrations of toxic metabolic by-products gradually increase within neurospheres as their size increases, compromising cell viability. To account for these effects a general mass transfer model which is similar to reaction-diffusion models of spherical catalysts can be considered as follows:

$$\frac{C}{t} = D \frac{d^2C}{r^2} + \frac{2D}{r} \frac{C}{r} - \frac{kXC}{K_m + C} \quad (1)$$

where  $k$  denotes oxygen uptake rate,  $X$  denotes viable cell density,  $D$  denotes diffusivity,  $C$  denotes concentration of oxygen and  $K_m$  denotes the Michaelis-Menten constant. Aggregate diameter was also approximated from its relationship to sphere volume, assuming spherical geometries in equation 2. This was required so that aggregate size could be passed on to the mass transfer model.

$$\text{Sphere volume} = \pi/6 (\text{Sphere diameter})^3 \quad (2)$$

Equation (1) can be solved numerically with appropriate boundary conditions and all the model parameters are determined experimentally. Once the values

of  $X$ ,  $k$ ,  $K_m$  and  $D$  are known, it is possible to incorporate the effects of oxygen mass transfer within aggregates into cellular automata model.

### Cell Lines, Media and Cell Culture

This work is conducted using a murine neural stem and progenitor cell lines, isolated from the striatal region of the forebrain of day 14 albino mouse embryos, as outlined by Reynolds and Weiss<sup>11</sup>. The medium, PPRF-m4, is a serum-free medium, is used for all relevant cell culture experiments. Filter-capped tissue culture flasks with 0.0075 m<sup>2</sup> surface area were used for all static cell cultures. While 125 mL bioreactor vessels (corning, cat. 26502-125) were used for suspension culture.

### Measurement of Oxygen Uptake Rate

The oxygen uptake rate of neural stem cells is determined by using a modified spinner flask bioreactor, which consisted of a sealed vessel with no headspace. The vessel has a volume of approximately 250 mL and a rubber lid with a hole for insertion of a dissolved oxygen (DO) probe. The impeller is agitated at 100 rpm and a known number of actively growing day 4 single cells/neurospheres are placed in the modified spinner with 250 mL of fresh 37°C PPRF-m4 medium. Immediately following this, the calibrated DO probe is inserted in the lid and the lid is securely placed into the vessel, cutting off access to the atmosphere (source of additional air). The DO measurements have to be recorded every minute using the Wheaton BIOPRO<sup>®</sup> software. The DO is

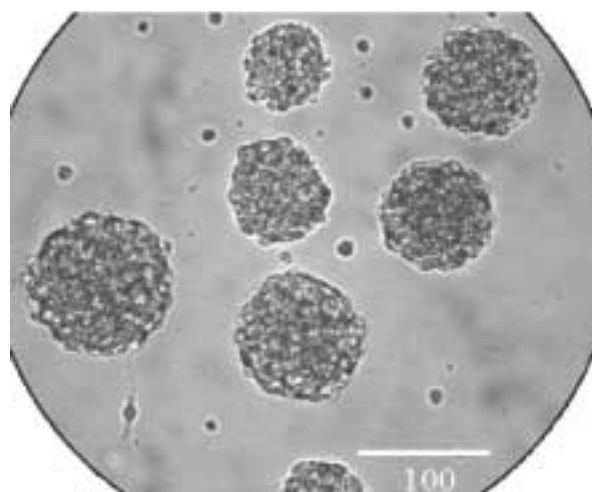


**Figure 9.** Photomicrograph of neural stem cell aggregates (neurospheres). Day-4 old cells were used to inoculate at a density 75,000 cells/mL in 125 mL spinner flasks. The cells were cultured at 37°C with 5% CO<sub>2</sub> in air.

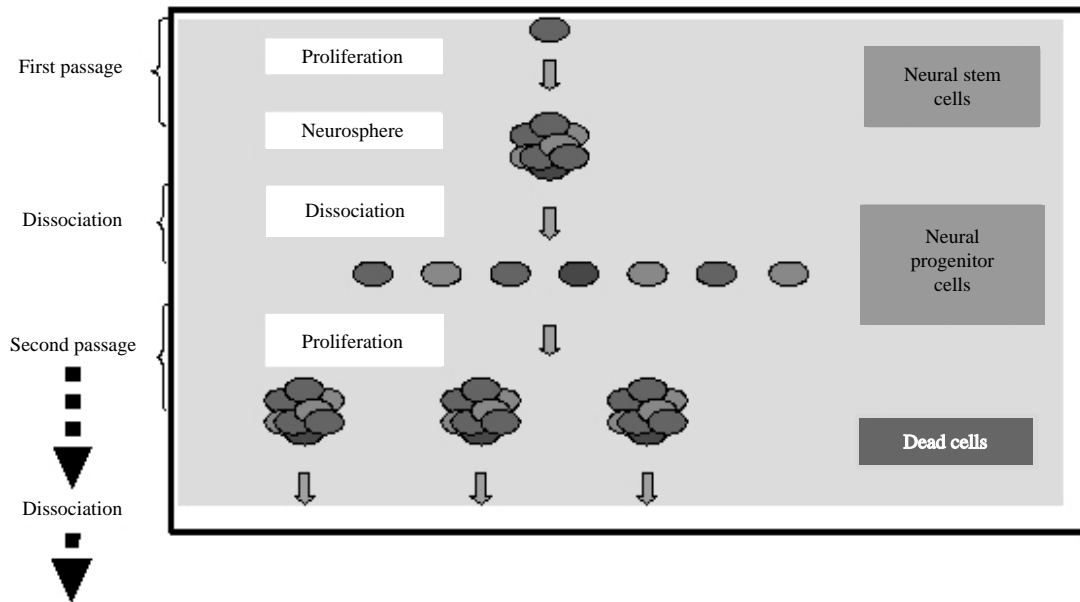


**Figure 10.** Schematic diagram of *In vitro* Expansion of Murine NSCs.

measured at specific time until the reading becomes zero. Oxygen uptake rate can then easily be determined from the slope of Dissolved Oxygen level (%) vs. time (min) plot.

### Measurement of Diffusivity of $O_2$ within Neurospheres

The diffusivity of oxygen within the neurospheres was calculated using the same data obtained to calculate the oxygen uptake rate of the neurospheres. First the average size of neurospheres diameter was determined by taking photographs of day-4 old cells culture. The diameter of approximately 200 neurospheres was calculated by measuring the horizontal and vertical diameters of each neurospheres and then averaging the two values. Then, the average of the 200 neurospheres diameters was taken as the average neurospheres diameter of that particular day. It was observed that on day-4 the majority of the neurospheres were 100  $\mu\text{m}$  in diameter (Figure 9). Therefore, to simplify the calculation of the diffusivity, all day-4 neurospheres were assumed to be 100  $\mu\text{m}$  in diameter. Then, theoretical oxygen uptake kinetics was determined by solving equation (1) numerically considering some appropriate boundary conditions. A value of diffusivity,  $D$  was estimated by fitting the resulting decline in oxygen concentration in the experimental apparatus,  $C$  to theoretical oxygen uptake kinetics.

### Population Analysis

A population study examines the ability of cells to

form new neurospheres. The ability of a single cell to proliferate and form a neurospheres is considered a validation that the cell is indeed a NSC<sup>12</sup>. Population analysis is carried out by inoculating 500 cells/200  $\mu\text{L}$ /well in a 96-wells plate and then counting the number of neurospheres formed after 6-8 days to calculate the sphere forming efficiency of the population. Figure 10 shows a general schematic diagram of *In vitro* expansion of murine NSCs. At the end of the population test, the total number of spheres formed is divided by the total number of single cells plated at the start of the test. This number is then multiplied by 100 and called the sphere forming efficiency which is considered as stem cells generation probability within neurospheres.

### Acknowledgements

The authors gratefully acknowledge the Pharmaceutical Production Research Facility (PPRF) laboratory, University of Calgary, Alberta, Canada for support of this work.

### References

1. Bailey, J. E. & Ollis, D. F. Biochemical engineering fundamentals. Second Edition, McGraw-Hill Company, Toronto (1986).
2. Berna, G., Leon, Q. T. & Martin, F. Stem cells and

- diabetes. *Biomed. Pharmacother.* **113**:206-212 (2001).
3. Blyszczuk, P. & Wobus, A. M. Stem cells and pancreatic differentiation *in vitro*. *J. of Biotechnology* **113**:3-13 (2004).
  4. Boucher, K., Yakovlev, A.Y., Mayer, P. M. & Noble, M. A stochastic model of temporally regulated generation of oligodendrocytes in cell culture. *Math. Biosci.* **159**:47-78 (1999).
  5. Boucher, K. *et al.* An alternative stochastic model of generation of oligodendrocytes in cell culture. *J. Math. Biol.* **43**:22-36 (2001).
  6. Cabrera, M. E., Saidel, G. M. & Kalhan, S.C. Role of O<sub>2</sub> in regulation of lactate dynamics during hypoxia: mathematical model and analysis. *Ann. Biomed. Eng.* **26**:1-27 (1998).
  7. Curry, J. L. & Trentin, J. J. Hemopoietic spleen colony studies. I. Growth and differentiation. *Dev. Biol.* **15**:395-413 (1967).
  8. Deasy, B. M. *et al.* Modeling stem cell population growth: incorporating terms for proliferative heterogeneity. *Stem Cells* **21**(5):536-545 (2003).
  9. Gilbertson, J. A., Sen, A., Behie, L. A. & Kallos, M. S. Scaled-up production of mammalian neural precursor cell aggregates in computer-controlled suspension bioreactors. *Biotechnology and Bioengineering* **94**(4):783-792 (2006).
  10. Metcalf, D. & Nicola, N. A. The regulatory factors controlling murine erythropoiesis *in vitro*. *Prog. Clin. Biol. Res.* **148**:93-105 (1984).
  11. Reynolds, B. A. & Weiss, S. Generation of neurons and astrocytes from isolated cells of the adult mammalian central nervous system. *Science* **255**:1707-1710 (1992).
  12. Reynolds, B. A. & Weiss, S. Clonal and population analyses demonstrate that an EGF-responsive mammalian embryonic CNS precursor is a stem cell. *Developmental Biology* **175**:1-13 (1996).
  13. Sadiq, T. S. & Gerber, D. A. Stem cells in modern medicine: reality or myth? *Journal of Surgical Research* **122**:280-291 (2004).
  14. Sen, A. & Behie, L. A. The development of a medium for the *in vitro* expansion of mammalian neural stem cells. *Canadian Journal of Chemical Engineering* **77**(5):963-972 (1999).
  15. Sen, A., Kallos, M. S. & Behie, L. A. Effect of hydrodynamics on cultures of mammalian neural stem cells aggregates in suspension bioreactors. *Industrial and Engineering Chemistry Research* **40**:5350-5357 (2001).
  16. Sen, A., Kallos, M. S. & Behie, L. A. Passaging protocols for mammalian neural stem cells in suspension bioreactors. *Biotechnology Progress* **18**(2):337-345 (2002a).
  17. Sen, A., Kallos, M. S. & Behie, L. A. Expansion of mammalian neural stem cells in bioreactors: Effect of power input and medium viscosity. *Developmental Brain Research* **134**(1-2):103-113 (2002b).
  18. Sen, A., Kallos, M. S. & Behie, L. A. New tissue dissociation protocol for scaled-Up production of neural stem cells in suspension bioreactors. *Tissue Engineering* **10**:904-913 (2004).
  19. Viswanathan, S. & Zandstra, P. W. Towards predictive models of stem cell fate. *Cytotechnology* **41**:75-92 (2003).
  20. Wang, T. Y., Sen, A., Behie, L. A. & Kallos, M. S. Dynamic behaviour of neurospheres in expanding populations of neural precursors. *Brain Research* **1107**:82-96 (2006).
  21. Yakovlev, A. Y., Mayer, P. M. & Noble, M. A stochastic model of brain cell differentiation in tissue culture. *J. Math. Biol.* **37**:49-60 (1998).
  22. Zhang, X. W., Audet, J., Piret, J. M. & Li, Y. X. Cell cycle distribution of primitive haematopoietic cells stimulated *in vitro* and *in vivo*. *Cell. Prolif.* **34**:321-330 (2001).
  23. Zorin, A., Mayer, P. M., Noble, M. & Yakovlev, A. Y. Estimation problems associated with stochastic modeling of proliferation and differentiation of O-2A progenitor cells *in vitro*. *Math. Biosci.* **167**:109-121 (2000).